# DAMAGE EVOLUTION OF DENSE NANOPILLARS LOCATED ON A TWO-DIMENSIONAL SQUARE GRID

***Tomasz Derda***

*Institute of Mathematics, Czestochowa University of Technology, Poland*
*tomasz.derda@im.pcz.pl*

**Abstract.** Stochastic approach is applied to study the mechanical damage accumulation occurring in an ensemble of elements located in the nodes of the supporting square lattice. The elements are treated as fibres in the framework of a Fibre Bundle Model and their strength thresholds are drawn from the Weibull probability distribution. Our example system is an array of densely packed nanopillars, which is subjected to increasing external load. After destruction of a pillar due to mechanical contact with its neighbours, the strength of the neighbours pillars increases. We study avalanches of the damaged pillars, critical loads causing system breakdown and distribution of load increments which triggers the avalanche.

## Introduction

The knowledge of fracture evolution up to the global rupture and its effective description are important for the analysis of the transport processes occurring in heterogeneous media. From the theoretical point of view, the understanding of the complexity of the rupture process has advanced due to the use of lattice models. An example of great importance is the family of transfer load models, especially Fibre Bundle Models (FBM) [1-12]. In a static FBM, a set of fibres is located in the nodes of the supporting lattice and the element strength thresholds are drawn from a given probability distribution. After an element has failed, its load has to be transferred to other intact elements.

Our paper is motivated by uniaxial tensile and compressive experiments on nano- and microscale materials that confirm substantial strength increase via the size reduction of the sample [13-18]. Especially studies on arrays of free-standing nanopillars subjected to uniaxial microcompression reveal the potential applicability of nanopillars as components for the fabrication of micro- and nano-electromechanical systems, micro-actuators or optoelectronic devices [13]. The aim of this contribution is to study the failure progress in an array of densely packed nanoscale metallic pillars. The pillars are vertically oriented and subjected to applied load. To illustrate the behaviour of the system, we map the array of nanopillars onto the surface with two-valued height function which corresponds to intact and damaged pillars.

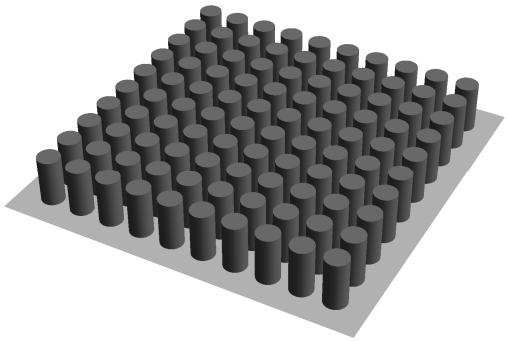

Fig. 1. An example of the set of nanopillars $N = 10\times10$ on the square lattice

## 1. Model

The system under consideration consists of $N = L \times L$ pillars located in the nodes of two dimensional square lattice of side length $L$, (see Fig. 1). To each pillar $x_i$ we assign an initial critical load $\sigma_{th}^{i}(\tau = 0)$, which is a strength threshold of the given pillar. $\tau$ is a time step. Initial strength thresholds $\sigma_{th}^{i}(\tau = 0)$, $i = 1,2,\ldots,N$ are identically distributed, independent random variables with the probability density and distribution functions: $p(\sigma_{th})$ and $P(\sigma_{th})$. It is assumed that the randomness of initial critical loads $\sigma_{th}^{i}(\tau = 0)$, $i = 1,2,\ldots,N$ represents the disorder of heterogeneous material. In this work we employ the Weibull distribution:

$$P(\sigma_{th}) = 1 - \exp\left[-\left(\frac{\sigma_{th}}{\lambda}\right)^{\rho}\right] \tag{1}$$

Here, the dimensionless number $\rho$ is the Weibull index and $\lambda$ is a scale parameter (setting the scale of the thresholds), which is fixed to $\lambda = 1$ in our study. The Weibull index controls the amount of disorder in the initial pillar strength-thresholds, so it is a very important parameter of the model. Probability density functions for different values of $\rho$ have been shown in Figure 2. As we can see from this Figure, the bigger the Weibull index $\rho$, the smaller the disorder.

The Weibull distribution is widely used in materials science, because conducted experiments proved that real materials follow very closely the Weibull probability distribution functions for strength of the individual elements [9]. It is assumed in materials science that the Weibull index takes values between 2 and 10 [10].

When load $\sigma_i$ applied on the pillar attains $\sigma_{th}^{i}$, the pillar instantaneously and irreversibly crashes.

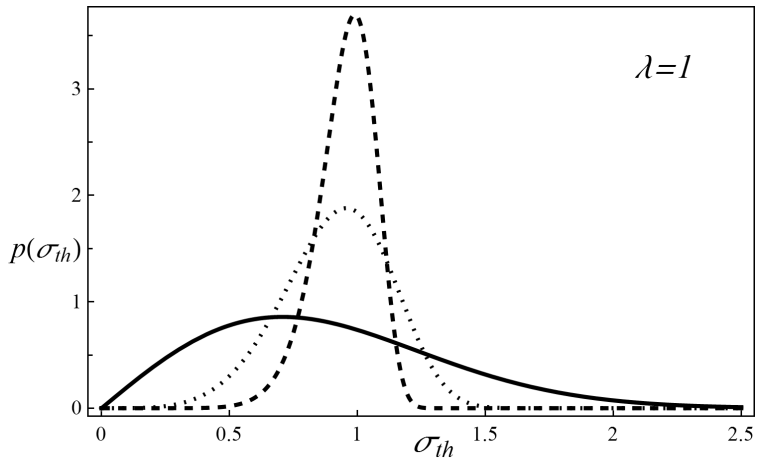


Fig. 2. The Weibull distribution with $\rho = 2$ (solid line), $\rho = 5$ (dotted line), $\rho = 10$ (dashed line)

## Loading of the system

At the beginning of the damage process all the pillars are intact. Then the system is loaded in a *quasi*-static way by an external force $F$ gently growing from its initial value $F = 0$. In this approach the damage process is controlled by the force $F$. The details of the process are as follows. External load $F$ is increased with a small amount $\delta\sigma$, so as to destroy the weakest intact pillar and the increase of load stops. After this failure the load dropped by the damaged pillar has to be redistributed to other intact pillars. For the load transfer we assume an infinite range of interaction, which is represented by global load sharing rule (GLS, also called equal load sharing - ELS). The increased stresses (loads) caused by the pillar destruction are shared equally among all intact pillars, so it means that all the intact elements are subjected to equal load. The increased stress on the intact pillars may give rise to other failures, after which the load transfer from the destroyed elements may cause subsequent failures. If the load transfer does not trigger further failures there is a stable configuration and external load $F$ has to be increased with a small amount $\delta\sigma$, just to provoke damage of the weakest intact pillar. By that means single failure induced by the load increment $\delta\sigma$ can cause an entire avalanche of failures. The above described procedure has to be repeated until the whole array of pillars collapses.

The novel ingredient of the model we consider here is that after failure of one pillar, its diameter grows giving rise to physical contact with remaining intact neighbours. As a consequence, these neighbouring pillars get higher strength thresholds $\sigma_{th}^{i}$ (see Fig. 3)

$$\sigma_{th}^{i}(\tau) = \sigma_{th}^{i}(\tau - 1) + n\delta \tag{2}$$

where $n$ is the number of these neighbours of the intact pillar $x_i$ which are destroyed during $\tau^{\text{th}}$ time step. The strength growth parameter $\delta$ is due to the friction appearing between the intact pillar and its deformed neighbour. Values of $\delta$ depend on many factors, as e.g. the surface of the pillar-pillar contacts or pillar inhomogeneities. In this paper we apply a simple statistical form of $\delta$ assuming that its range is expressed as the fraction of the mean initial strength threshold averaged over the entire system

$$\delta = \eta \langle \sigma_{th} \rangle . \tag{3}$$

Here, the factor $\eta$ is a strengthening coefficient and $\langle \sigma_{th} \rangle = N^{-1} \sum \sigma_{th}^{i}(0)$ is the mean initial strength threshold of the system. The appearance of the higher strength-thresholds $\{\sigma_{th}^{i}\}$ is schematically shown in Figure 4.

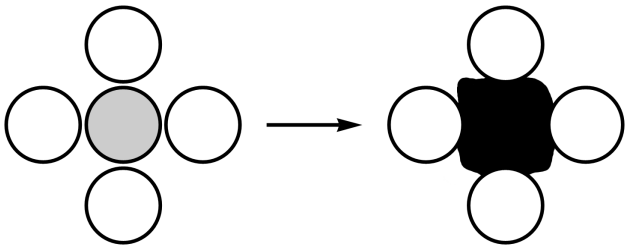

Fig. 3. Destruction of the pillar. Grey disk - before destruction, black figure - after destruction

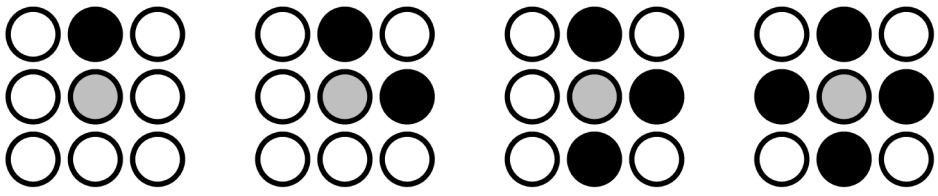


Fig. 4. Strengthening of the intact pillar (grey disk) in dependence on the number of just destroyed neighbouring pillars. Black disks indicate just damaged pillars

In the following part of this work we will call the model without the novel ingredient a classical model of nanopillars.

## 2. Characteristics of the damage process

Our simulations were realised on $N = 10^4$ pillars for different values of $\rho$ and $\eta$. In order to obtain reliable statistics we have performed at least $10^3$ simulations for each values of $\rho$ and $\eta$. We are interested in a few undermentioned quantities.

The damage process is characterised by the distribution of the size of avalanches, $\Delta$ being the number of destroyed pillars under an equal external load. Here, the avalanche is the number of crashed pillars between one stable state two successive. Each avalanche is triggered by the load increment $\delta\sigma$. Both the avalanche size $\Delta$ and the load increment $\delta\sigma$ are random variables.

Another quantity describing the damage process is the total critical load $F_c$, which causes a complete breakdown of the system. The critical load $F_c$ triggers a catastrophic (fatal) avalanche $\Delta_{fa}$, i.e. a final avalanche breaking all the remaining intact pillars and causing a macroscopic failure of the entire system, so it is the final stage of the breakdown process.

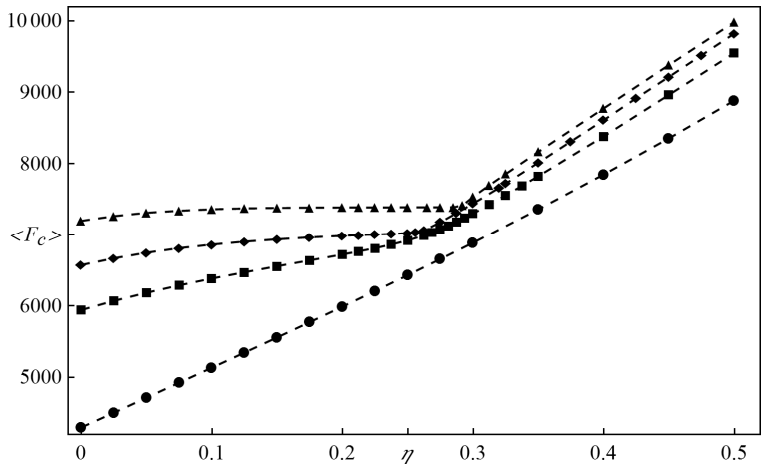


Fig. 5. Mean critical force vs. strengthening coefficient $\eta$ for different values of the Weibull index $\rho$: $\rho$ = 2 (circles), $\rho$ = 5 (squares), $\rho$ = 7 (diamonds), $\rho$ = 10 (triangles)

Figure 5 shows dependence between mean total critical loads $\langle F_c \rangle$ and values of strengthening coefficient $\eta$ for different values of the Weibull index. Systems with a big disorder of initial strength thresholds $(\rho = 2)$ are characterized by nearly linear growth of mean critical loads with increasing values of $\eta$. For weakly disordered systems $(\rho = 10)$ two regimes can be seen: first, in which values of $\langle F_c \rangle$ slowly increase or even does not change with the increase of $\eta$ (from $\eta = 0.0$ to $\eta \approx 0.3$) and second, when values of critical load increase like for strongly disordered case (from $\eta \approx 0.3$ to $\eta = 0.5$). On average, a system with small disorder $(\rho = 10)$ can sustain almost equal values of critical load from $\eta \approx 0.15$ to

$\eta \approx 0.28$ . We also observe that for systems $2 < \rho < 10$ the mean critical load curve is concave for $\eta < 0.3$ and then it grows almost linearly (see Fig. 5). From Figure 5 it is also seen that the bigger the Weibull index, the stronger the system. This ordering is preserved for consecutive values of $\eta$, however the difference between system strength varies for each $\eta$ .

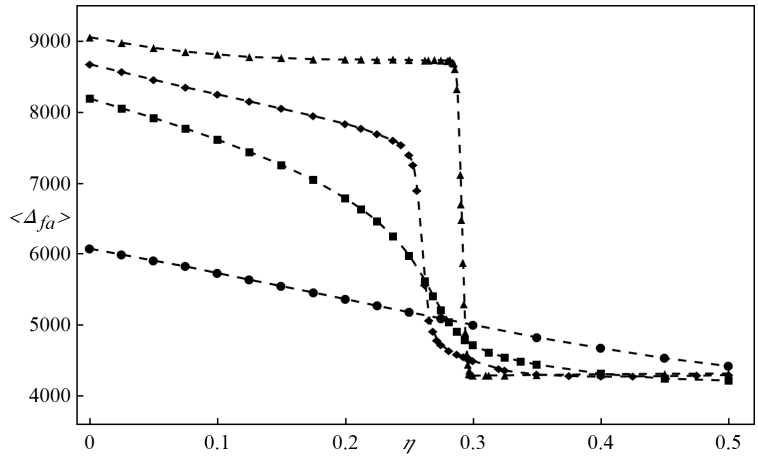


Fig. 6. Mean size of catastrophic avalanche vs. strengthening coefficient $\eta$ for different values of the Weibull index $\rho$: $\rho$ = 2 (circles), $\rho$ = 5 (squares), $\rho$ = 7 (diamonds), $\rho$ = 10 (triangles)

Dependence between mean sizes of catastrophic avalanche and values of the strengthening coefficient is illustrated Figure 6. On average with catastrophic avalanche sizes for systems with a big disorder $(\rho = 2)$ decrease almost linearly with growing coefficient $\eta$. Systems with medium disorder of strength thresholds $(\rho = 5$ and $\rho = 7)$ are also characterised by decreasing catastrophic avalanche with increasing coefficient $\eta$, but this decrease is different in comparison with the strongly disordered system. In these cases smooth decrease of $\langle \Delta_{fa} \rangle$ is followed by its rapid drop and subsequently next smooth decrease. For weakly disordered systems $(\rho = 10)$ after small decrease of $\langle \Delta_{fa} \rangle$ with increasing $\eta$, there is a rapid drop of $\langle \Delta_{fa} \rangle$ for $\eta \approx 0.29$ and thereafter values of $\langle \Delta_{fa} \rangle$ nearly do not change with an increase of $\eta$. Mean catastrophic avalanche sizes $\langle \Delta_{fa} \rangle$ for $\eta \approx 0.29$ and $\rho = 10$ range from 8730 to 4300, according to the percentage of long and short catastrophic avalanches in the all samples for a particular $\eta$. In the analysed range of $\eta$ it can be seen that the most resistant system to changes of $\langle \Delta_{fa} \rangle$ is the strongly disordered one.

In order to get a closer look at the sizes of catastrophic avalanches for values of $\eta$ near rapid drop of $\langle \Delta_{fa} \rangle$ we have chosen a weakly disordered system $(\rho = 8)$ with $\eta = 0.27$. Figure 7 shows empirical probability distribution of catastrophic avalanche sizes for this system. As it can be noticed, the distribution is multimodal with two main different modes. It means that the catastrophic avalanche may take sizes around the two main modes: $\Delta_{fa} = 4616$ (63.7% of results) and $\Delta_{fa} = 8279$ (34.69% of results). There is also a small probability that the catastrophic avalanche has the size around third mode $\Delta_{fa} = 5856$ (1.61% of results). In our simulations we received multimodal distribution of catastrophic avalanche sizes within the range from $\eta \approx 0.265$ to $\eta \approx 0.273$ with $\rho = 8$. Systems with $\rho = 10$ are characterised by bimodal distribution of $\Delta_{fa}$ within the range from $\eta \approx 0.287$ to $\eta \approx 0.295$.

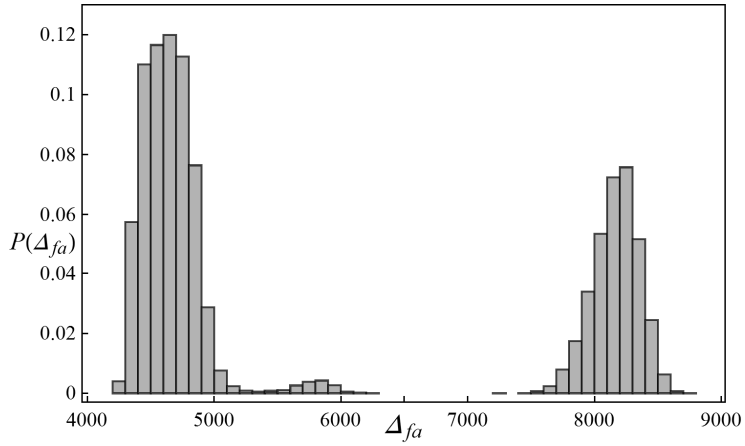


Fig. 7. Empirical probability distribution of catastrophic avalanche sizes for systems with Weibull index 8 and strengthening coefficient $\eta = 0.27$. The simulation results are based on 20000 samples, each containing $N = 10^4$ pillars

In the following we built up a distribution of total critical loads $F_c$, triggering catastrophic avalanches $\Delta_{fa}$ for systems with $\rho = 8$ and $\eta = 0.27$ (see Fig. 8). In this case critical loads $F_c$ are characterised by unimodal distribution with mean $\mu = 7155.01$, standard deviation $s = 19.3847$, skewness $g_1 = 0.3263$ and kurtosis $g_2 = 3.1633$. The dependence between the size of the catastrophic avalanche $\Delta_{fa}$ and the total critical load $F_c$ (for system with $\rho = 8$ and $\eta = 0.27$) has been shown in Figure 9. As it can be seen, critical loads of similar values may trigger catastrophic avalanches in three distinct size intervals and, on the other hand, criti-

cal loads of different values cause system breakdown with catastrophic avalanches of similar size. This means that $F_c$ and $\Delta_{fa}$ are uncorrelated.

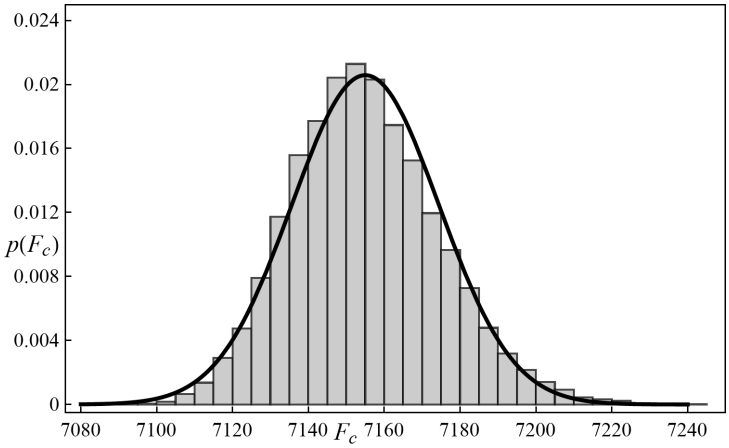


Fig. 8. Empirical probability density distribution of total critical loads for systems with the Weibull distributed strength values ($\rho = 8$) and strengthening coefficient $\eta = 0.27$. The simulation results are based on 20000 samples, each containing $N = 10^4$ pillars. Solid line - probability density function of normal distribution with mean $\mu = 7155.01$ and standard deviation $s = 19.3847$

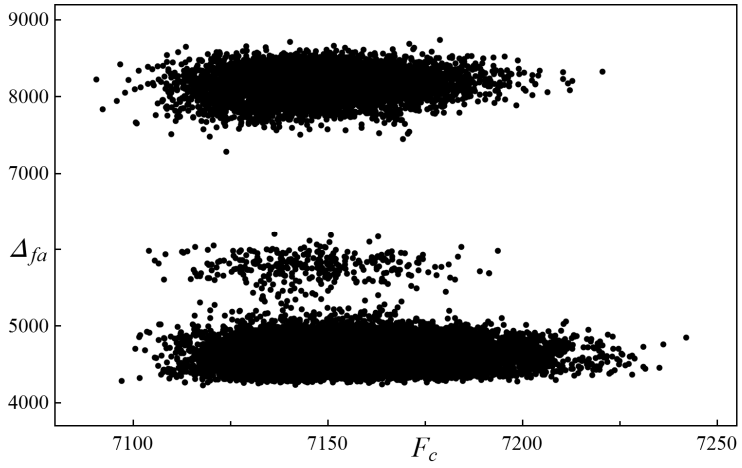


Fig. 9. The size of the final catastrophic avalanche vs. the total critical force for systems with Weibull index $\rho = 8$ and strengthening coefficient $\eta = 0.27$. The simulation results are based on 20000 samples, each containing $N = 10^4$ pillars

The distribution of avalanche sizes for classical model has a universal power law decay:

$$D(\Delta) \propto \Delta^{-\alpha} \tag{4}$$

where the value of the exponent $\alpha = 5/2$ is independent of the disorder distribution $P$ [2;4;5;12]. In this work we analyse avalanche size distribution for chosen cases of systems of contacting dense nanopillars.

In Figure 10 we compare avalanche size distribution $D(\Delta)$ for system with Weibull index $\rho = 5$ and three different values of $\eta$. It can be noticed that $D(\Delta)$ for these systems also exhibits power law behaviour with slightly different values of exponent $\alpha$. With increasing $\eta$ the number of non-fatal avalanches grows. It is related with decreasing size of the catastrophic avalanche (see Fig. 6). For the sake of clarity the catastrophic avalanches are omitted in Figure 10.

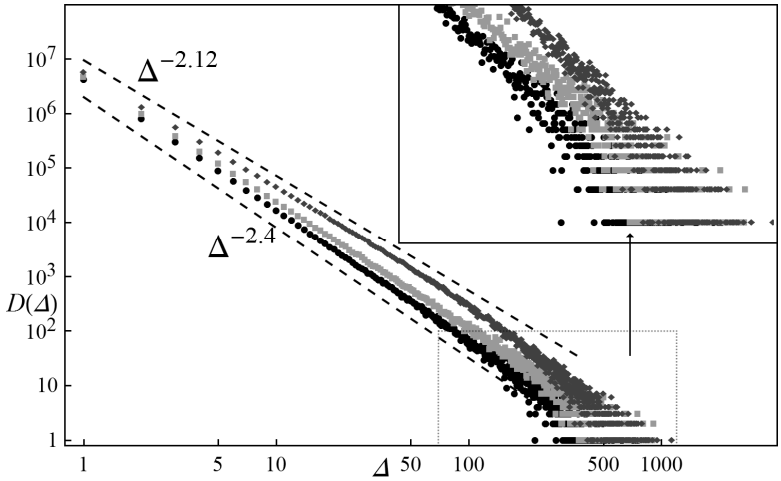


Fig. 10. Avalanche size distributions for systems with the Weibull index $\rho$ = 5 and different values of strengthening coefficient: $\eta$ = 0.1(black circles), $\eta$ = 0.2 (light grey squares), $\eta$ = 0.3 (dark grey diamonds). The simulation results are based on 5000 samples, each containing $N = 10^4$ pillars

Another example is a weakly disordered system with $\rho = 10$. Comparison between avalanche size distribution for the classical system and a system with $\eta = 0.3$ has been shown in Figure 11. Here catastrophic avalanches are not presented. For systems with $\eta = 0.3$ the frequency of non-fatal avalanches is significantly increased in comparison with the classical systems. In contrast to the classical models, in 99.97% of simulations during damage process of the system with $\eta = 0.3$ a long non-fatal avalanche occurs. In our simulations these avalanches have taken sizes from the interval [3181,4697] with probability distribution presented in Figure 12. Long non-fatal avalanche is followed by series of next shorter non-fatal avalanches, including the avalanche of the order of 300 pillars (in 84% of simulations it has a length from the interval [100, 600]), before system breakdown.

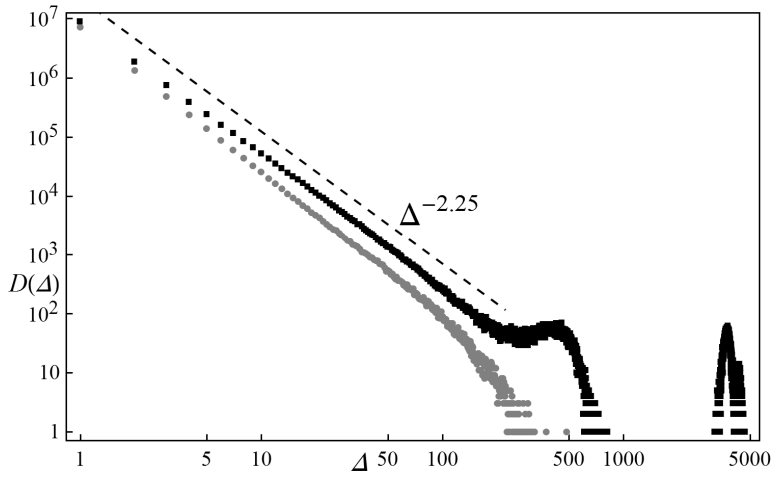


Fig. 11. Avalanche size distributions for the systems with the Weibull index $\rho$ = 10: a model with strengthening coefficient $\eta$ = 0.3 (black squares) compared with a classical model (grey circles). The simulation results are based on 20000 samples, each containing $N = 10^4$ pillars

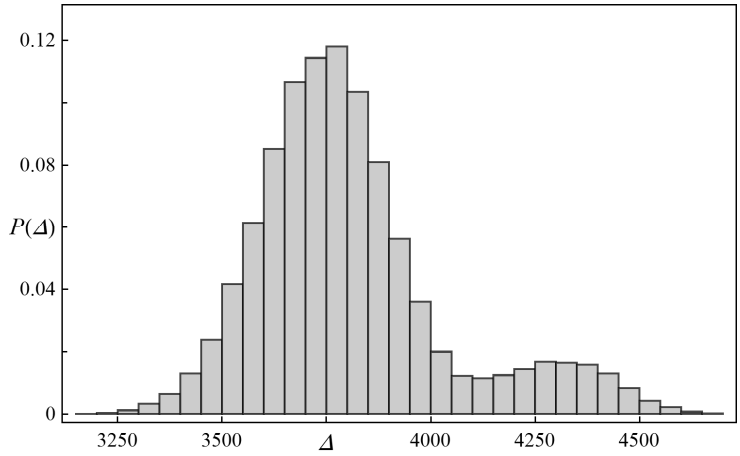


Fig. 12. Empirical probability distribution of long non-fatal avalanches for the system with $\rho$ = 10 and $\eta$ = 0.3. The simulation results are based on 20 000 samples, each containing $N = 10^4$ pillars

Computer simulations revealed that distribution of discrete load increments $D(\delta\sigma)$ follows a power law behaviour

$$D(\delta\sigma) \propto \delta\sigma^{-\beta} \tag{5}$$

Figure 13 presents the distribution of load increments for systems with $\rho = 5$ and $\eta = 0.2$. Approximate values of exponent $\beta$ are shown in Table 1.

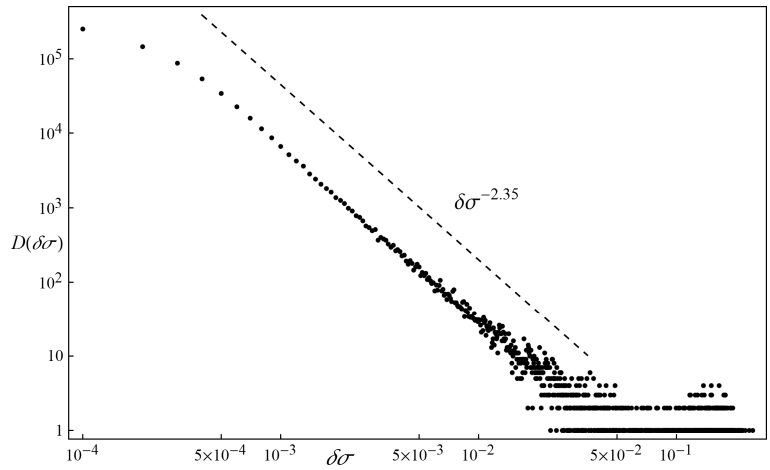


Fig. 13. The distribution of load increments $D(\delta\sigma)$ which trigger the avalanches for systems with the Weibull index $\rho = 5$ and strengthening coefficient $\eta = 0.2$. The simulation results are based on 500 samples, each containing $N = 10^4$ pillars

Table 1

**Approximate values of exponent $\beta$ - formula (5)**

| Strengthening coefficient | The Weibull index | | |
|---|---|---|---|
| | $\rho = 2$ | $\rho = 5$ | $\rho = 10$ |
| $\eta = 0.0$ | 3.05 | 2.2 | 2.1 |
| $\eta = 0.1$ | 3.1 | 2.3 | 2.1 |
| $\eta = 0.2$ | 3.1 | 2.35 | 2.1 |
| $\eta = 0.3$ | 3.2 | 2.4 | 2.2 |

## Conclusions

In summary, we have studied damage process of *quasi*-statically loaded sets of dense nanopillars. These sets are characterised by strength increase of intact neighbours of destroyed pillars. Our simulations have been performed for different degrees of system disorder. We have noticed a strength increase of the whole system with a growing strengthening coefficient for the individual pillars. Damage evolution can be described by avalanches of destroyed pillars. We find that power law decay of avalanche distribution, seen in the classical models, remains, but with somewhat different exponents. With growing strengthening coefficient the number of non-fatal avalanches increases (especially for more disordered systems), therefore the size of catastrophic avalanche decreases. Changes of system strength and size of catastrophic avalanches are sensitive to the amount of system disorder. For

instance, the sizes of catastrophic avalanches in systems with small disorder change abruptly around certain value of strengthening coefficient.

We showed that for some values of strengthening coefficient and weakly disordered systems the distribution of avalanche sizes is multimodal. The distribution of load increments, triggering avalanches, exhibits power law behaviour.

## References

[1] Herrmann H.J., Roux S. (eds.), Statistical Models for the Fracture of Disordered Media, North Holland, Amsterdam 1990 and references therein.

[2] Alava M.J., Nukala P.K.V.V., Zapperi S., Statistical models of fracture, Advances in Physics 2006, 55, 349-476.

[3] Pradhan S., Hansen A., Chakrabarti B.K., Failure processes in elastic fiber bundles, Rev. Mod. Phys. 2010, 82, 499-555.

[4] Hemmer P.C., Hansen A., The Distribution of simultaneous fiber failures in fiber bundles, ASME J. Appl. Mech. 1992, 59, 909-914.

[5] Raischel F., Kun F., Herrmann H.J., Fiber Bundle Models for Composite Materials, Conference on Damage in Composite Materials 2006, Stuttgart 2006.

[6] Pradhan S., Hansen A., Hemmer P.C., Burst statistics as a criterion for imminent failure, IUTAM Bookseries 2009, 10, 165-175.

[7] Hemmer P.C., Hansen A., Pradhan S., Rupture processes in fiber bundle models, Lecture Notes in Physics 2006, 705, 27-55.

[8] Halasz Z., Kun F., Slip avalanches in a fiber bundle model, EPL 2010, 89, 26008.

[9] Vazquez-Prada M., Gomez J.B., Moreno Y., Pacheco A.F., Time to failure of hierarchical load-transfer models of fracture, Phys. Rev. E 1999, 60, 2581-2594.

[10] Gomez J.B., Vazquez-Prada M., Moreno Y., Pacheco A.F., Bounds for the time to failure of hierarchical systems of fracture, Phys. Rev. E. 1999, 59, R1287.

[11] Derda T., Domański Z., Damage evolution on two-dimensional grids - comparison of load transfer rules, Scientific Research of the Institute of Mathematics and Computer Science 2010, 1(9), 5-15.

[12] Derda T., Avalanche statistics in transfer load models od evolving damage, Scientific Research of the Institute of Mathematics and Computer Science 2011, 1(10), 21-31.

[13] Greer J.R., Jang D., Kim J.-Y., Burek M.J., Emergence of new mechanical functionality in materials via size reduction, Adv. Functional Materials 2009, 19, 2880-6.

[14] Brinckmann S., Kim J.-Y., Greer J.R., Fundamental differences in mechanical behaviour between two types of crystals at the nanoscale, Phys. Rev. Letters 2008, 100, 155502.

[15] Jang D., Greer J.R., Transition from a strong-yet-brittle to a stronger-and-ductile state by size reduction of metallic glasses, Nature Materials 2010, 9, 215-219.

[16] Uchic M.D., Dimiduk D.M., Florando J.N., Nix W.D., Sample dimensions influence strength and crystal plasticity, Science 2004, 305, 986-989.

[17] Shan Z.W., Mishra R., Syed Asif S.A., Warren O.L., Minor A.M, Mechanical annealing and source-limited deformation in submicron-diameter Ni crystals, Nature Materials 2008, 7, 115-119.

[18] Huang L., Li Q.-J., Shan Z.-W., Li J., Sun J., Ma E., A new regime for mechanical annealing and strong sample-size strengthening in body centered cubic molybdenum, Nature Communications 2011, 2.